Available online at www.sciencedirect.com

ScienceDirect

Current Opinion in Chemical Biology

High-speed atomic force microscopy

Toshio Ando

High-speed atomic force microscopy (HS-AFM) is a unique tool for molecular imaging. It can directly visualize protein molecules during their functional activity at high spatiotemporal resolution, without a marker being attached to the molecules. Molecular dynamics filmed with HS-AFM can provide mechanistic insights into the functional molecular processes that are hard to be attained with other approaches. In this mini review, I highlight some of recent relevant studies of proteins by HS-AFM imaging after brief descriptions of AFM and HS-AFM.

Address
Nano Life Science Institute (WPI-NanoLSI), Kanazawa University, Kakuma-machi, Kanazawa 920-1192, Japan

Corresponding author: Ando, Toshio (tando@staff.kanazawa-u.ac.jp)

Current Opinion in Chemical Biology 2019, **51**:105–112

This review comes from a themed issue on **Molecular imaging**

Edited by **Philipp Kukura** and **Sua Myong**

For a complete overview see the Issue and the Editorial

Available online 27th June 2019

https://doi.org/10.1016/j.cbpa.2019.05.010

Introduction

In AFM imaging of biological samples, a micro-cantilever with a sharp tip at its free end is excited to oscillate at its first resonant frequency. The oscillating tip intermittently contacts with the sample surface, resulting in alteration of the cantilever's oscillation amplitude. The cantilever deflection is detected with an optical beam deflection detector, in which a laser beam reflected back from the cantilever illuminates a position-sensitive photodetector. The laser spot on the photodetector moves up and down as the cantilever oscillates. During the raster-scanning of the sample stage in the XY direction, the cantilever oscillation amplitude (and hence, the tip-sample interaction force) is held constant by moving the sample stage in the Z-direction via feedback control. Consequently, the sample stage movement traces the sample surface. The feedback signal that is proportional to the Z-scanner displacement is used to form a topography image of the sample surface. Note that the intermittent tip-sample contact avoids the sample being dragged laterally by the tip. Because of the chasing-after nature of feedback control, the tip-sample interaction force cannot be perfectly held constant but varies; this feedback error becomes larger with increasing XY-scan speed. To minimize the error under fast scanning, the response speed of all components contained in the feedback loop has to be increased. To this end, various devices and techniques have been developed [1,2•], including short (7–10 μm) cantilevers with a high resonant frequency in water and a small spring constant [1,3,4], a dynamic feedback controller enabling the minimization of AFM-tip impact on the sample during fast scanning [5], and some others [2•]. Through these long-term efforts, HS-AFM for biomolecular imaging was established in 2008. The feedback bandwidth (FB) of our system, which determines the system's speed performance, is about 110 kHz when it is used together with a short cantilever with resonant frequency of 1.2 MHz in water. The highest possible imaging rate depends not only on FB but also on imaging parameters (e.g. the scan range and the number of scan lines) and sample fragility [6]. In our system, it is typically ~15 frames/s (fps) in imaging individual protein molecules without retarding their function [6]. Currently, devices limiting FB are the Z-scanner and the amplitude detector. The employment of a new amplitude detection method [7] and recent advanced piezo actuators has a potential to increase the imaging rate up to 60–80 fps. HS-AFM systems and short cantilevers are now commercially available, although their speed performance largely varies among the products.

HS-AFM has been used for not only imaging proteins but also live cell imaging [8,9], chemically oriented studies on DNA/RNA [10,11], mechanical measurements of cells and biopolymers [12•,13], and others. However, in this mini review I focus on HS-AFM imaging of proteins (other than transmembrane proteins). For HS-AFM imaging of transmembrane proteins, see the recent review [14•].

HS-AFM studies during 2010–2014

Even before the establishment of HS-AFM technology in 2008, HS-AFM imaging was performed on proteins, DNA and lipid membranes to test and explore the capability of HS-AFM systems under development (most of these studies are listed in [15•]). During 2010–2014, a few molecular processes including dynamic structural changes and dynamic interactions in protein systems were successfully filmed with HS-AFM, as reviewed in Ref. [16••]. Among these studies, the work on dynamic processes of myosin V walking on actin filaments is a milestone in the history of biomolecular imaging [17••]. This study provided a new view for the force generation and usage of ATP energy in myosins. HS-AFM imaging of the $\alpha_3\beta_3$ subcomplex (stator ring) of F_1-ATPase also led to a surprising discovery [18•]. It revealed that the three different chemical (and structural) states rotated over

the three β subunits, indicating that the γ subunit is passively subjected to torque to rotate. This finding predicted that objects completely different from the γ subunit might be able to rotate when they were inserted into the central cavity of the $\alpha_3\beta_3$ ring. This prediction was confirmed later for F_1-ATPase [19], and similarly for V_1-ATPase [20].

HS-AFM studies during 2015–2019

During the last four years and a few months, the number of publications of HS-AFM imaging of proteins was abruptly increased (more than 60), compared to the previous five years. This is due partly to the increased number of HS-AFM users and the increased number of their collaborators convinced of the power of HS-AFM. The targeted proteins range from ion channels [21–24] to membrane-transforming proteins [25,26•,27••], molecular chaperones including assembly chaperones [28•,29,30], enzymes including cas9, proteasome and protein disulfide isomerase [31–37], cytoskeletons [38–40], DNA binding proteins [41,42], pore-forming toxins [43–45], clock proteins [46], protein exporters [47], motor proteins [48,49], intrinsically disordered proteins including amyloid-related proteins [50–52], bacterial cell division-controlling proteins MinDE [53], and even to the nuclear pore complex [54,55]. Five studies among these are highlighted below.

ESCRT-III proteins

The endosomal sorting complexes required for transport (ESCRT) are involved in various processes that need lipid membrane remodelling and scission, including multivesicular body biogenesis, cytokinesis and viral budding [56]. Among ESCRT complexes, the filamentous ESCRT-III complex, consisting of core subunits, Vps20, Snf7, Vps2, and Vps24, plays an essential role in membrane deformation and scission together with the AAA + ATPase Vps4. Unlike other membrane-remodelling proteins such as dynamin, ESCRT-III propels outward membrane budding. The endogenous ESCRT-III filaments in Vps4-depleted cells were observed as conical spirals by electron microscopy [57]. ESCRT-III filaments are mainly formed by polymerization of its main component, Snf7, on the membrane. Indeed, HS-AFM imaging of Snf7 showed that it polymerizes into concentric rings and spirals on the surface of lipid bilayers [26•]. When they were disrupted by the cantilever tip, the broken polymers spontaneously formed smaller rings, suggesting a preferred curvature (25–30 nm radius) for Snf7 polymers. Since the polymers grow into larger spirals, they accumulate tension like a spiral spring. Thus, it was postulated that in cellular conditions unbend strain (and energy) would be accumulated during the growth of the spiral spring and eventually released through shrinking of the spiral diameter and buckling of the inner spirals, causing the membrane to buckle, bud and undergo abscission [26•]. To examine this idea in more realistic conditions, HS-AFM imaging and fluorescence imaging were performed in the presence of Snf7, Vps2, and Vps24 [27••]. Vps2/Vps24 were observed as lateral copolymers along Snf7, thickening the polymers, and more importantly stalled the growth and accumulation of Snf7 polymers. HS-AFM imaging in the presence of Snf7, Vps2, Vps24, the ATPase Vsp4 and ATP, Snf7 concentric rings and spirals were observed to undergo dynamic reorganization (growth and shrinking) by subunit turnover (Figure 1 shows spiral disassembly), and finally reach a dynamic steady state. This dynamics was not observed without Vsp4 and ATP, and thus, the subunit turnover is fueled with ATP turnover. Although these results have enriched our knowledge of dynamic events occurring in this system, it is still elusive how these events result in membrane transformation and scission.

Chaperonin GroEL

This bacterial molecular chaperone with a double-ring structure assists proper folding of many proteins, in cooperation with the co-chaperonin, GroES, which binds to the ends of GroEL cylinder depending on the nucleotide state of GroEL [58]. The dynamic GroEL–GroES interaction reflects the allosteric intra-ring and inter-ring communications and the chaperonin reaction. Therefore, revealing this dynamic interaction is essential to understanding these fundamental

Figure 1

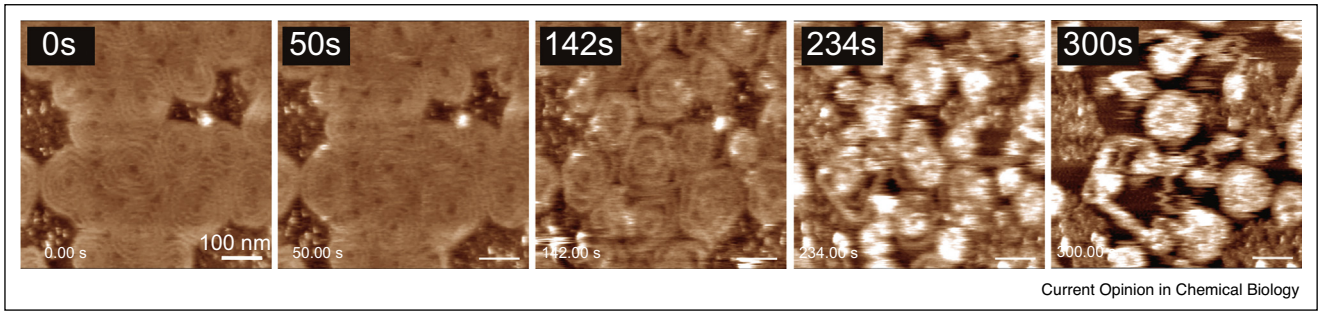

HS-AFM images showing disassembly of ESCRT-III spirals caused by the ATPase reaction of Vps4. The spiral assemblies were formed by polymerization of Snf7, followed by binding of Vps2 and Vps24 to the spiral polymers. After all soluble components were washed out, Vps4 was injected. Then, ATP and Mg^{2+} were added and imaging was started 22 s later ($t = 0$). Imaging rate, 0.25 fps.

issues. Nevertheless, these issues have long been controversial. This is mostly because of a lack of technique capable of identifying at which ring GroES binding and release are taking place during chaperonin cycles. For HS-AFM imaging, D490C GroEL mutant biotinylated at Cys490 was tethered in a side-on orientation onto the 2D crystal surface of a tamavidin 2 mutein [28•]. The filmed images led to new findings and thereby provided new insights into the molecular processes. It was revealed that the GroEL–GroES interaction proceeds mainly in the order of B↑ → F → B↓ → F, where B and F represent asymmetric GroEL:$GroES_1$ (bullet) and symmetric GroEL:$GroES_2$ (football) complexes, respectively, and the vertical arrows represent the polarity of bullet complexes. That is, in the main pathway of a cycle time of ~5 s GroES binding and release take place alternately between the two rings (Figure 2a). This alternate rhythm was disrupted at a relatively large frequency (25–33%), resulting in branching into the side pathway, B↑ → F → B↑ → F, with a cycle time of ~3 s (Figure 2b). From the analysis of residence time of bound GroES in the main pathway, how the two rings communicate with each other was revealed (Figure 2c). Strikingly, the timing of ATP hydrolysis into ADP–Pi in a *cis*-ring coincides with the timing of ADP release from the opposite *trans*-ring. Therefore, the ATP hydrolysis works as a timer to control the timing of ADP release from the opposite ring. This communication is functionally important; it ensures the release of substrate protein from the *trans*-ring before it is capped with GroES. A recent biochemical study for GroEL mutants reported a striking result that the two rings of GroEL separate and exchange between complexes [59]. However, this separation did not appear in the HS-AFM images, possibly due to the tethering of GroEL to the surface. The ring separation and exchange will be directly visualized with HS-AFM.

Molecular chaperone ClpB

This AAA + molecular chaperone and its yeast homolog Hsp104 disentangle and reactivate aggregated proteins [60]. HS-AFM images of ClpB hexamers in the presence of ATP showed a variety of conformations from round and

Figure 2

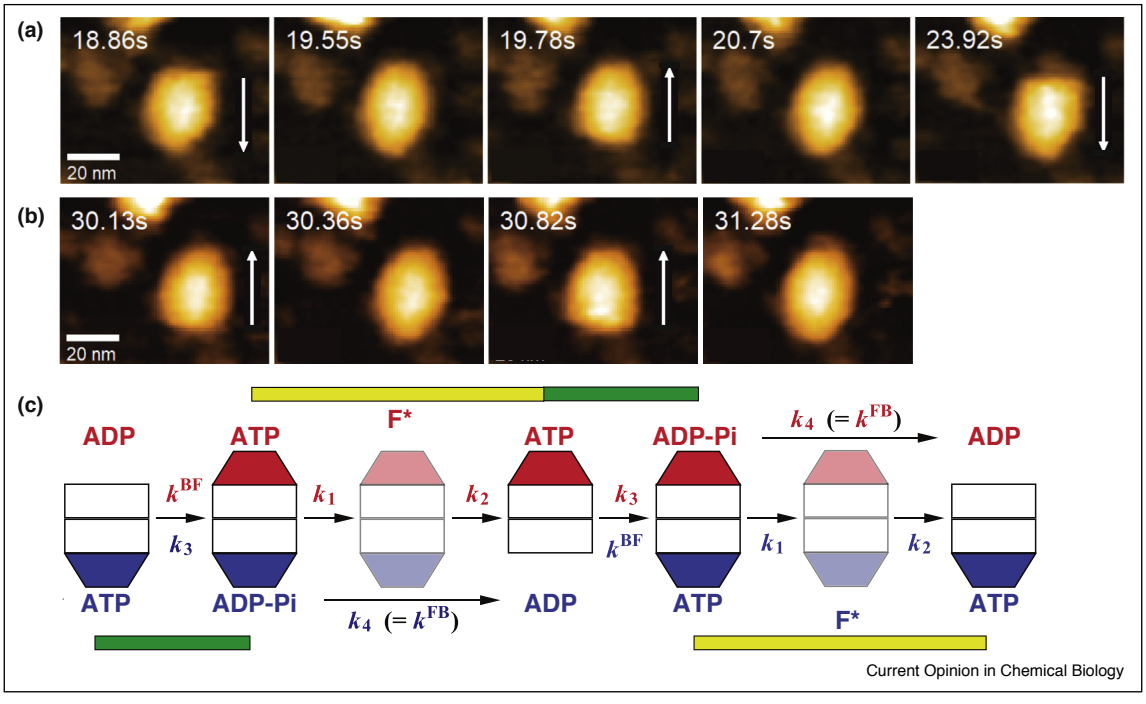

HS-AFM images showing dynamic binding and release of GroES at the two rings of GroEL in the presence of denatured rhodanese and Mg^{2+}–ATP. Imaging rate, 4.3 fps. The vertical arrows show the polarity of bullet complexes **(a, b)**. **(a)** HS-AFM images showing alternate polarity changes in bullet complexes appearing in the main pathway of chaperonin reaction. **(b)** HS-AFM images showing non-alternate polarity changes in bullet complexes appearing in the side pathway of chaperonin reaction. **(c)** Kinetic scheme of main reaction pathway and inter-ring communications revealed by lifetime analyses of intermediate states appeared in HS-AFM images. The nucleotide states, GroES binding and release, and rate constants in transitions occurring in the top and bottom rings are shown in red and blue, respectively. The football complexes (F*) shown in pale colors are apparently the same as but kinetically different from the football complexes formed immediately before. Analysis of GroES residence time distribution provided the values of four rate constants, k_1, k_2, k_3, and k_4, leading to a new finding of two coincidences: $1/k_1 + 1/k_2 = 1/k^{FB}$ (marked with the yellow bars) and $k_3 = 1/k^{BF}$ (marked with the green bars). The latter coincidence indicates a functionally important inter-ring communication; ATP hydrolysis into ADP–Pi in *cis*-ring triggers ADP release from the opposite *trans*-ring. Note that ATP binding and subsequent GroES binding occur immediately after ADP release (since the ATP and GroES concentrations used are nearly saturated), and therefore, ADP dissociation limits the B-to-F transition rate.

Figure 3

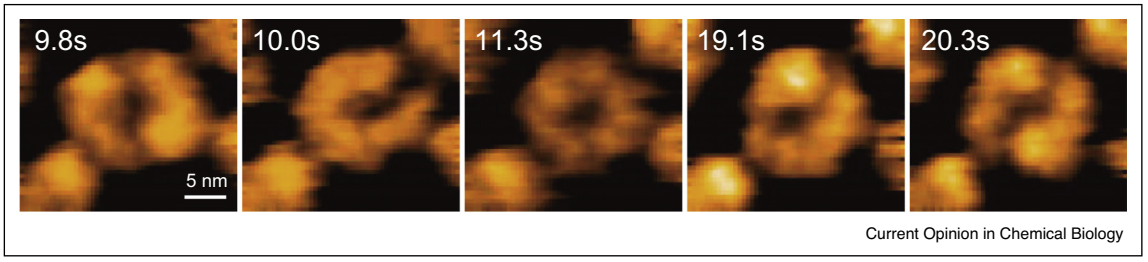

HS-AFM images showing massive conformational changes of ΔN-ClpB during the ATPase reaction. Different structures appeared, including a twisted-half-spiral ring (9.8 s, 20.3 s), a round ring (11.3 s), a spiral ring (10.0 s), and an intermediate between spiral and twisted-half spiral rings (19.1 s). Imaging rate, 10 fps.

spiral rings to twisted-half-spiral rings, and even to open rings [29] (Figure 3). The twisted-half-spiral form (dimer of trimers) was identified in this study for the first time. These conformations were observed to transform from one to another during the ATPase cycle, with a frequency similar to the ATPase rate per hexamer. These structural changes were drastically decreased in a middle-domain mutant that lost disaggregation activity but retained ATPase activity. Thus, ClpB performs protein disaggregation through these structural changes, in particular through large height increase in the spiral and twisted-half spiral rings, which possibly acts to extend and disentangle aggregated proteins trapped in their central cavity. Moreover, individual roles of the two ATPase cores, AAA1 and AAA2, were clarified by HS-AFM imaging of ClpB mutants. ATP binding to the AAA1 domain induces oligomerization of ClpB, and the hexameric state is stabilized by ATP binding to the AAA2 domain. The structural changes between different ring forms are caused by ATP hydrolysis on the AAA2 domain. Note that the structural analysis of ClpB is considerably difficult with other methods, since ClpB conformations are populated among the four types as well as their subtypes.

Bacterial rotary motor's stator MotPS

Some bacteria possess two types of flagella rotary motors that are driven by a transmembrane electrochemical gradient of either N^+ or H^+ ions [61]. The motors are switched on/off depending on the ionic environment where bacteria inhabit in. However, this switching mechanism has long been elusive. This fundamental question was quickly solved by HS-AFM imaging of an amphipol-dissolved MotPS protein complex from *Bacillus*, which functions as a stator of the Na^+-driven rotary motor [49]. The images captured in the presence of N^+ ions showed a larger globule connected to a smaller globule through a flexible linker (Figure 4, 0–10.5 s). The larger and smaller globules correspond to the transmembrane region of the MotPS complex and the peptidoglycan biding region of MotS, respectively. When the ionic condition was changed from Na^+ to K^+, the smaller globule was unfolded into mobile chains (Figure 4). This structural change was reversed when the ionic condition was changed from K^+ to Na^+. Thus, it was clearly revealed that the transitions between ordered and disordered conformations of the peptidoglycan binding region of MotS are responsible for switch on/off of the Na^+-driven flagella motor.

Figure 4

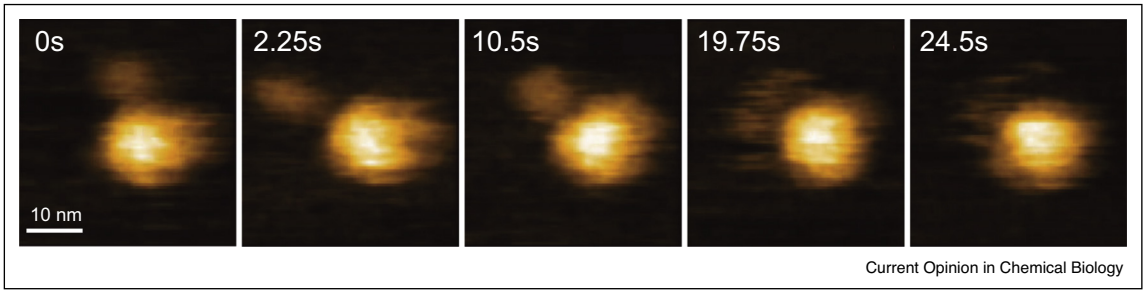

HS-AFM images showing unfolding of the peptideglycan layer binding domain of MotS upon displacement of Na^+ with K^+. The MotPS complex was solubilized with amphipol. The large globule corresponds to the transmembrane domain of MotPS containing MotP and the N-terminal domain of dimeric MotS. The small globule corresponds to the C-terminal domain of dimeric MotS containing the peptideglycan layer binding region. These two globules are linked through a flexible unstructured chain. At 19.75 s, the C-terminal domain of MotS is unfolded, exhibiting its fast diffusional motion. Imaging rate, 4 fps.

Figure 5

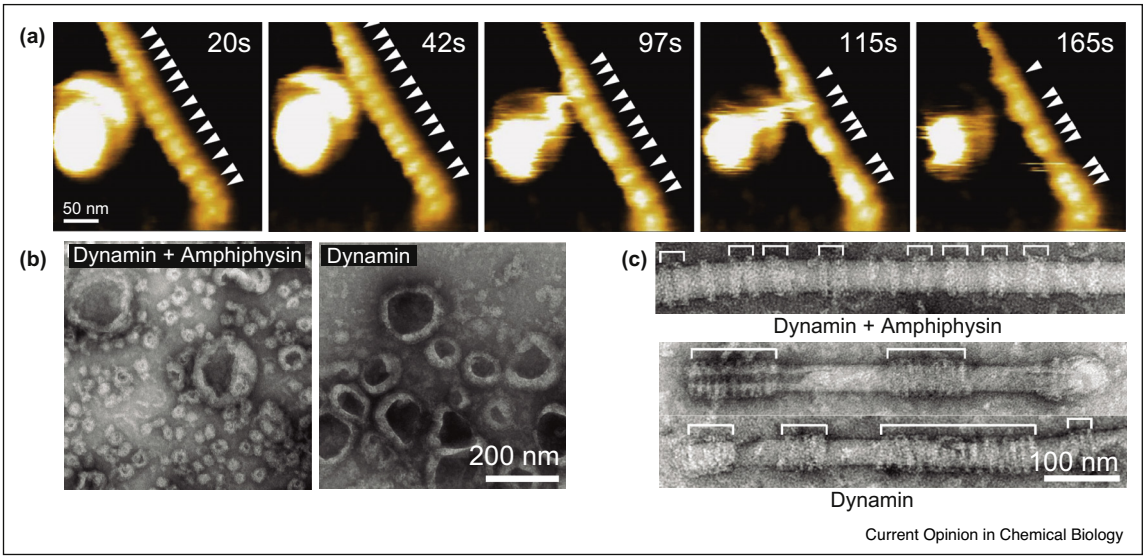

HS-AFM images and electron micrographs (EMs) showing clustering of lipid tube-surrounding dynaminn helices. **(a)** HS-AFM images showing dynamic clustering of lipid tube-surrounding dynamin–amphiphysin helices in the presence of GTP. 1 mM GTP was added at 42 s. After clustering of dynamin–amphiphysin helices, their helical pitch was narrowed from 22.0 nm (before GTP addition) to 15.7 nm. Bare zones in the lipid tube between protein clusters became thinner at 165 s. Imaging rate, 1 fps. **(b)** EMs showing membrane vesicles formed by dynamin–amphiphysin and dynamin alone in the presence of GTP. **(c)** EMs showing amphiphysin-dependence of dynamin ring clusters formed around rigid lipid nanotubes containing glycolipid galactosylceramide in the presence of GDP and vanadate.

Membrane fission protein dynamin

In neuronal synapses, synaptic vesicles containing neurotransmitters are fused with the presynaptic terminal membrane, resulting in the release of neurotransmitters to the synaptic gap. To recycle membranes for preparing synaptic vesicles again, clathrin-mediated endocytosis takes place at the presynaptic terminal [62]. A GTPase, dynamin, works together with a BAR domain protein, amphiphysin, to produce an inwardly budded membrane tube by forming a spiral complex around the membrane, and then GTP hydrolysis by dynamin results in membrane fission, producing membrane vesicles. Several mechanisms have been postulated for membrane fission by dynamin [63]. However, any model has never been proven experimentally. HS-AFM imaging was performed for membrane tubes surrounded by spiral oligomers of dynamin–amphiphysin complexes [25], leading to a new mechanistic insight into membrane fission by dynamin. Upon addition of GTP, the regularly packed dynamin–amphiphysin complexes in a spiral form were disrupted, resulting in the formation of regions possessing clustered dynamin–amphiphysin complexes and bare membrane regions lacking the proteins (Figure 5a). Remarkably, membrane constrictions were observed at the bare membrane regions, and the diameter of the bare regions were getting smaller with time. Interestingly, the volume of the membrane area underneath each dynamin–amphiphysin cluster was similar to that of presynaptic vesicles. EM observations of membrane vesicles produced by dynamin–amphiphysin complexes in the presence of GTP confirmed this volume size coincidence. Membrane vesicles were also produced by dynamin alone in the presence of GTP but the vesicle size was much larger than those produced by dynamin–amphiphysin (Figure 5b). Consistent with this result, the size of dynamin clusters formed upon the addition of GDP and vanadate was also much larger than that of dynamin–amphiphysin clusters (Figure 5c). From these observations, it was put forward that a pair of neighboring dynamin–amphiphysin clusters twists the bare membrane region between them. This twist causes membrane fission at the bare region, resulting in isolation and release of protein-clustered regions from the membrane tube, followed by dissociation of dynamin–amphiphysin from the released protein–vesicle complex. Nonetheless, it is still elusive how a pair of neighboring dynamin–amphiphysin clusters twists the bare zone and why the membrane tube undergoes scission by this twist despite fast diffusion of lipids.

Conclusion

Before the advent of HS-AFM, the protein structure revealed was only static snapshots, while dynamic events observed were only those of an optical maker attached to proteins. Large gaps have therefore remained in our understanding of dynamic molecular processes occurring during the functional activity of proteins. The spatiotemporal resolution of HS-AFM is moderate but it provides a

unique opportunity of assessing structure and dynamics simultaneously. The power of this new assessment has been demonstrated by growing number of HS-AFM imaging studies carried out mostly on purified protein systems. The functionality of HS-AFM is now being expanded. One of newly added functions is sample manipulation with controlled strong tip-force application to operator-specified loci of the sample during successive imaging. This technique was recently used to break the high molecular weight complexes of peroxiredoxin, leading to a discovery of the involvement of negatively charged lipids in the structural and functional conversion of this protein [31]. This technique also revealed that two inner-lumen proteins of doublet microtubules (MT) in *Chlamydomonas* flagella stabilize MT against force-induced depolymerization of MT [64•]. Tip-scan HS-AFM is already developed and combined with fluorescence microscopy [65], facilitating AFM imaging of the surfaces of live cells [66•] and isolated organelles. The next targets of this combined system would be dynamic molecular processes occurring in the interior of de-roofed cells [67•]. Although not yet established, HS-AFM combined with optical tweezers will enable observing protein molecules under an external force; unfolding/refolding processes and motor proteins under backward/forward forces. Moreover, the temporal resolution of HS-AFM will be improved at least 4-times (~15 ms) in the near future. Thus, HS-AFM will further open new dimensions in bioimaging.

Conflict of interest statement

Nothing declared.

Acknowledgements

This work was supported by Grant-in-Aids for Basic Research S (#17H06121 to T.A.), Grant-in-Aids for Research on Innovative Area (#26119003 to T.A.) and a CREST program of Japan Science and Technology Agency(#JPMJCR13M1 to T.A.).

References and recommended reading

Papers of particular interest, published within the period of review, have been highlighted as:

- • of special interest
- •• of outstanding interest

1. Ando T, Kodera N, Takai E, Maruyama D, Saito K, Toda A: **A high-speed atomic force microscope for studying biological macromolecules**. *Proc Natl Acad Sci U S A* 2001, **98**: 12468-12472.

2. • Ando T, Uchihashi T, Fukuma T: **High-speed atomic force microscopy for nano-visualization of dynamic biomolecular processes**. *Prog Surf Sci* 2008, **83**:337-437.
A great review describing various techniques underlying HS-AFM.

3. Viani MB, Schäffer TE, Paloczi GT, Pietrasanta LI, Smith BL, Thompson JB, Richter M, Rief M, Gaub HE, Plaxco KW *et al.*: **Fast imaging and fast force spectroscopy of single biopolymers with a new atomic force microscope designed for small cantilevers**. *Rev Sci Instrum* 1999, **70**:4300.

4. Kitazawa M, Shiotani K, Toda A: **Batch fabrication of sharpened silicon nitride tips**. *Jpn J Appl Phys* 2003, **42**:4844.

5. Kodera N, Sakashita M, Ando T: **Dynamic proportional-integral-differential controller for high-speed atomic force microscopy**. *Rev Sci Instrum* 2007, **77**:083704.

6. Ando T, Uchihashi T, Kodera N: **High-speed AFM and applications to biomolecular systems**. *Annu Rev Biophys* 2013, **42**:393-414.

7. Miyagi A, Scheuring S: **A novel phase-shift-based amplitude detector for a high-speed atomic force microscope**. *Rev Sci Instrum* 2018, **89**:083704.

8. Shibata M, Uchihashi T, Ando T, Yasuda R: **Long-tip high-speed atomic force microscopy for nanometer-scale imaging in live cells**. *Sci Rep* 2015, **5**:8724.

9. Fantner GE, Barbero RJ, Gray DS, Belcher AM: **Kinetics of antimicrobial peptide activity measured on individual bacterial cells using high-speed atomic force microscopy**. *Nat Nanotechnol* 2010, **5**:280-285.

10. Endo M, Sugiyama H: **Single-molecule imaging of dynamic motions of biomolecules in DNA origami nanostructures using high-speed atomic force microscopy**. *Acc Chem Res* 2014, **47**:1645-1653.

11. Takeuchi Y, Endo M, Suzuki Y, Hidaka K, Durand G, Dausse E, Toulmé JJ, Sugiyama H: **Single-molecule observations of RNA-RNA kissing interactions in a DNA nanostructure**. *Biomater Sci* 2016, **4**:130-135.

12. • Rigato A, Miyagi A, Scheuring S, Rico F: **High-frequency microrheology reveals cytoskeleton dynamics in living cells**. *Nat Phys* 2017, **13**:771-775.
A representative study of HS-AFM application for high-frequency force spectroscopy.

13. Rico F, Gonzalez L, Casuso I, Puig-Vidal M, Scheuring S: **High-speed force spectroscopy unfolds titin at the velocity of molecular dynamics simulations**. *Science* 2013, **342**:741-743.

14. • Heath GR, Scheuring S: **Advances in high-speed atomic force microscopy (HS-AFM) reveal dynamics of transmembrane channels and transporters**. *Curr Opin Struct Biol* 2019, **57**: 93-102.
A nice review highlighting HS-AFM imaging of transmembrane proteins.

15. • Ando T: **High-speed atomic force microscopy coming of age**. *Nanotechnology* 2012, **23**:062001.
A nice review of history of HS-AFM technology development.

16. •• Ando T, Uchihashi T, Scheuring S: **Filming biomolecular processes by high-speed atomic force microscopy**. *Chem Rev* 2014, **114**:3120-3188.
A great review highlighting HS-AFM applications performed before 2014.

17. •• Kodera N, Yamamoto D, Ishikawa R, Ando T: **Video imaging of walking myosin V by high-speed atomic force microscopy**. *Nature* 2010, **468**:72-76.
A milestone work of biomolecular imaging showing unprecedented details of myosin V walking and tension generation.

18. • Uchihashi T, Iino R, Ando T, Noji H: **High-speed atomic force microscopy reveals rotary catalysis of rotorless F_1-ATPase**. *Science* 2011, **333**:755-758.
A representative study of HS-AFM applications making a surprising discovery from structural changes of rotorless F_1-ATPase filmed by HS-AFM.

19. Chiwata R, Kohori A, Kawakami R, Shiroguchi K, Furuike S, Adachi K, Sutoh K, Yoshida M, Kinosita K Jr: **None of the rotor residues of F_1-ATPase are essential for torque generation**. *Biophys J* 2014, **106**:2166-2174.

20. Baba M, Iwamoto K, Iino R, Ueno H, Hara M, Nakanishi A, Kishikawa J, Noji H, Yokoyama K: **Rotation of artificial rotor axles in rotary molecular motors**. *Proc Natl Acad Sci U S A* 2016, **113**:11214-11219.

21. Marchesi A, Gao X, Adaixo R, Rheinberger J, Stahlberg H, Nimigean C, Scheuring S: **An iris diaphragm mechanism to gate a cyclic nucleotide-gated ion channel**. *Nat Commun* 2018, **9**:3978.

22. Ruan Y, Kao K, Lefebvre S, Marchesi A, Corringer P-J, Hite RK, Scheuring S: **Structural titration of receptor ion channel GLIC**

gating by HS-AFM. *Proc Natl Acad Sci U S A* 2018, **115**: 10333-10338.

23. Rangl M, Miyagi A, Kowal J, Stahlberg H, Nimigean C, Scheuring S: **Real-time visualization of conformational changes upon ligand unbinding from single MloK1 cyclic nucleotide-modulated channels**. *Nat Commun* 2016, **7**:12789.

24. Horner A, Zocher F, Preiner J, Ollinger N, Siligan C, Akimov SA, Pohl P: **The mobility of single-file water molecules is governed by the number of H-bonds they may form with channel-lining residues**. *Sci Adv* 2015, **1**:e1400083.

25. Takeda T, Kozai T, Yang H, Ishikuro D, Seyama K, Kumagai Y, Abe T, Yamada H, Uchihashi T, Ando T, Takei K: **Dynamic clustering of dynamin-amphiphysin helices regulates membrane constriction and fission coupled with GTP hydrolysis**. *eLife* 2018, **7**:e30246.

26. • Chiaruttini N, Redondo-Morata L, Colom A, Humbert F, Lenz M, Scheuring S, Roux A: **Relaxation of loaded ESCRT-III spiral springs drives membrane deformation**. *Cell* 2015, **163**:866-879.
A nice work showing the usefulness of sample manipulation with AFM tip during HS-AFM imaging.

27. •• Mierzwa B, Chiaruttini N, Redondo-Morata L, von Filseck JM, König J, Larios J, Poser I, Müller-Reichert T, Scheuring S, Roux A, Gehrlich D: **Dynamic subunit turnover in ESCRT-III assemblies is regulated by Vps4 to mediate membrane remodeling during cytokinesis**. *Nat Cell Biol* 2017, **19**:787-798.
A great work showing the usefulness of combining multiple approaches including HS-AFM in solving important biological questions in complex biomolecular systems.

28. • Noshiro D, Ando T: **Substrate protein dependence of GroEL-GroES interaction cycle revealed by high-speed AFM imaging**. *Philos Trans R Soc B* 2018, **373**:20170180.
A representative work showing the power of HS-AFM to reveal the entire scheme of very complex kinetic reactions.

29. Uchihashi T, Watanabe Y, Nakazaki Y, Yamasaki T, Watanabe H, Maruno T, Ishii K, Uchiyama S, Song C, Murata K *et al.*: **Dynamic structural states of ClpB involved in its disaggregation function**. *Nat Commun* 2018, **9**:2147.

30. Yagi-Utsumi M, Sikdar A, Kozai T, Inoue R, Sugiyama M, Uchihashi T, Satoh T, Kato K: **Conversion of functionally undefined homopentameric protein PbaA into a proteasome activator by mutational modification of its C-terminal segment conformation**. *Protein Eng Des Sel* 2018, **31**:29-36.

31. Haruyama T, Uchihashi T, Yamada Y, Kodera N, Ando T, Konno H: **Negatively charged lipids are essential for functional and structural switch of human 2-Cys peroxiredoxin II**. *J Mol Biol* 2018, **430**:602-610.

32. Shibata M, Nishimasu H, Kodera N, Hirano S, Ando T, Uchihashi T, Nureki O: **Real-space and real-time dynamics of CRISPR-Cas9 visualized by high-speed atomic force microscopy**. *Nat Commun* 2017, **8**:1430.

33. Watanabe-Nakayama T, Itami M, Kodera N, Ando T, Konno H: **High-speed atomic force microscopy reveals strongly polarized movement of clostridial collagenase along collagen fibrils**. *Sci Rep* 2016, **6**:28975.

34. Harada H, Onoda A, Uchihashi T, Watanabe H, Sunagawa N, Samejima M, Igarashi K, Hayashi T: **Interdomain flip-flop motion visualized in flavocytochrome cellobiose dehydrogenase using high-speed atomic force microscopy during catalysis**. *Chem Sci* 2017, **8**:6561-6565.

35. Benning FMC, Sakiyama Y, Adam M, Habib BST, Roderick LYH, Timm M: **High-speed atomic force microscopy visualization of the dynamics of the multienzyme fatty acid synthase**. *ACS Nano* 2017, **11**:10852-10859.

36. Kozai T, Sekiguchi T, Satoh T, Yagi H, Kato K, Uchihashi T: **Two-step process for disassembly mechanism of proteasome α7 homo-tetradecamer by α6 revealed by high-speed atomic force microscopy**. *Sci Rep* 2017, **7**:15373.

37. Okumura M, Noi K, Kanemura S, Kinoshita M, Saio T, Inoue Y, Hikima T, Akiyama S, Ogura T, Inaba K: **Dynamic assembly of protein disulfide isomerase in catalysis of oxidative folding**. *Nat Chem Biol* 2019, **15**:499-509.

38. Keya JJ, Inoue D, Suzuki Y, Kozai T, Ishikuro D, Kodera N, Uchihashi T, Kabir AMR, Endo M, Sada K, Kakugo A: **High-resolution imaging of a single gliding protofilament of tubulins by HS-AFM**. *Sci Rep* 2017, **7**:6166.

39. Ngo KX, Kodera N, Katayama E, Ando T, Uyeda TQP: **Cofilin-induced unidirectional cooperative conformational changes in actin filaments revealed by high-speed AFM**. *eLife* 2015, **4**: e04806.

40. Ganser C, Uchihashi T: **Microtubule self-healing and defect creation investigated by in-line force measurements during high-speed atomic force microscopy**. *Nanoscale* 2019, **11**:125-135.

41. Sun Z, Hashemi M, Warren G, Bianco PR, Lyubchenko YL: **Dynamics of the interaction of RecG protein with stalled replication forks**. *Biochemistry* 2018, **57**:1967-1976.

42. Eeftens JM, Katan AJ, Kschonsak M, Hassler M, de Wilde L, Dief EM, Haering CH, Dekker C: **Condensin smc2-smc4 dimers are flexible and dynamic**. *Cell Rep* 2016, **14**:1813-1818.

43. Munguira I, Takahashi H, Casuso I, Scheuring S: **Lysenin toxin membrane insertion is pH-dependent and non-cooperative**. *Biophys J* 2017, **113**:2029-2036.

44. Kisovec M, Rezelj S, Knap P, Cajnko MM, Caserman S, Flašker A, nidaršič N, Repič M, Mavri J, Ruan Y *et al.*: **Engineering a pH responsive pore forming protein**. *Sci Rep* 2017, **7**:42231.

45. Morante K, Bellomio A, Gil-Cartón D, Redondo-Morata L, Sot J, Scheuring S, Valle M, González-Mañas JM, Tsumoto K, Caaveiro JMM: **Identification of a membrane-bound prepore species clarifies the lytic mechanism of actinoporins**. *J Biol Chem* 2016, **291**:19210-19219.

46. Mori T, Sugiyama S, Byme M, Johnson CH, Uchihashi T, Ando T: **Revealing circadian mechanisms of integration and resilience by visualizing clock proteins working in real time**. *Nat Commun* 2018, **9**:3245.

47. Terahara N, Inoue Y, Kodera N, Morimoto YV, Uchihashi T, Imada K, Ando T, Namba K, Minamino T: **Insight into structural remodeling of the FlhA ring responsible for bacterial flagellar type III protein export**. *Sci Adv* 2018, **4**:eaao7054.

48. Davies T, Kodera N, Schierle GSK, Rees E, Erdelyi M, Kaminski CF, Ando T, Mishima M: **CYK4 promotes antiparallel microtubule bundling by optimizing MKLP1 neck conformation**. *PLoS Biol* 2015, **13**:e1002121.

49. Terahara N, Kodera N, Uchihashi T, Ando T, Namba K, Minamino T: **Na+-induced structural transition of MotPS for stator assembly of the *Bacillus* fragellar motor**. *Sci Adv* 2017, **3**: eaao4119.

50. Yamamoto H, Fujioka Y, Suzuki SW, Noshiro D, Suzuki H, Kondo-Kakuta C, Kimura Y, Hirano H, Ando T, Noda NN, Ohsumi Y: **The intrinsically disordered protein Atg13 mediates supramolecular assembly of autophagy initiation complexes**. *Dev Cell* 2016, **38**:86-99.

51. Zhang Y, Hashemi M, Lv Z, Williams B, Popov KI, Dokholyan NV, Lyubchenko YL: **High-speed atomic force microscopy reveals structural dynamics of α-synuclein monomers and dimers**. *J Chem Phys* 2018, **148**:123322.

52. Watanabe-Nakayama T, Ono K, Itami M, Takahashi R, Teplow DB, Yamada M: **High-speed atomic force microscopy reveals structural dynamics of amyloid β1-42 aggregates**. *Proc Natl Acad Sci U S A* 2016, **113**:5835-5840.

53. Miyagi A, Ramm B, Schwille P, Scheuring S: **High-speed AFM reveals the inner workings of the MinDE protein oscillator**. *Nano Lett* 2018, **18**:288-296.

54. Yusuke S, Adam M, Kapinos LE, Lim RYH: **Spatiotemporal dynamics of the nuclear pore complex transport barrier resolved by high-speed atomic force microscopy**. *Nat Nanotechnol* 2016, **11**:719-723.

55. Mohamed MS, Kobayashi A, Taoka A, Watanabe-Nakayama T, Kikuchi Y, Hazawa M, Minamoto T, Fukumori Y, Kodera N, Uchihashi T *et al.*: **High-speed atomic force microscopy reveals**

loss of nuclear pore resilience as a dying code in colorectal cancer cells. *ACS Nano* 2017, **11**:5567-5578.

56. Schöneberg J, Lee IH, Iwasa JH, Hurley JH: **Reverse-topology membrane scission by the ESCRT proteins**. *Nat Rev Mol Cell Biol* 2017, **18**:5-17.

57. Cashikar AG, Shim S, Roth R, Maldazys MR, Heuser JE, Hanson PI: **Structure of cellular ESCRT-III spirals and their relationship to HIV budding**. *eLife* 2014, **3**:e02184.

58. Horwich AL, Fenton WA: **Chaperonin-mediated protein folding: using a central cavity to kinetically assist polypeptide chain folding**. *Q Rev Biophys* 2009, **42**:83-116.

59. Yan X, Shi Q, Bracher A, Miličić G, Singh AK, Ulrich Hartl F, Hayer-Hartl M: **GroEL ring separation and exchange in the chaperonin reaction**. *Cell* 2018, **172**:605-617.

60. Doyle SM, Wickner S: **Hsp104 and ClpB: protein disaggregating machines**. *Trends Biochem Sci* 2008, **34**:40-48.

61. Ito M, Terahara N, Fujinami S, Krulwich TA: **Properties of motility in *Bacillus subtilis* powered by the H+-coupled MotAB flagellar stator, Na+-coupled MotPS or hybrid stators MotAS or MotPB**. *J Mol Biol* 2005, **352**:396-408.

62. Rizzoli SO: **Synaptic vesicle recycling: steps and principles**. *EMBO J* 2014, **33**:788-822.

63. Morlot S, Roux A: **Mechanics of dynamin-mediated membrane fission**. *Annu Rev Biophys* 2013, **42**:629-649.

64. • Owa M, Uchihashi T, Yanagisawa H, Yamano T, Iguchi H, Fukuzawa H, Wakabayashi K, Ando T, Kikkawa M: **Inner lumen proteins stabilize doublet microtubules in cilia and flagella**. *Nat Commun* 2019, **10**:1143.
A nice work showing the usefulness of sample manipulation with an AFM tip during successive HS-AFM imaging.

65. Uchihashi T, Watanabe H, Fukuda S, Shibata M, Ando T: **Functional extension of high-speed atomic force microscopy**. *Ultramicroscopy* 2016, **160**:182-196.

66. • Yoshida A, Sakai N, Uekusa Y, Imaoka Y, Itagaki Y, Suzuki Y, Yoshimura SH: **Morphological changes of plasma membrane and protein assembly during clathrin-mediated endocytosis**. *PLoS Biol* 2018, **16**:e2004786.
A representative work showing the power of simultaneous fluorescence and HS-AFM imaging.

67. • Usukura E, Narita A, Yagi A, Ito S, Usukura J: **An unroofing method to observe the cytoskeleton directly at molecular resolution using atomic force microscopy**. *Sci Rep* 2016, **6**:27472.
A nice work showing a future direction of HS-AFM imaging (cell interior imaging)